Materials Science in Semiconductor Processing 80 (2018) 52–55

Contents lists available at ScienceDirect

Materials Science in Semiconductor Processing

journal homepage: www.elsevier.com/locate/mssp

Photoluminescence study of deep donor- deep acceptor pairs in Cu_2ZnSnS_4

J. Krustok[a,b,*], T. Raadik[b], M. Grossberg[b], M. Kauk-Kuusik[b], V. Trifiletti[c], S. Binetti[c]

[a] Division of Physics, Tallinn University of Technology, Ehitajate Tee 5, 19086 Tallinn, Estonia
[b] Department of Materials and Environmental Technology, Tallinn University of Technology, Ehitajate Tee 5, 19086 Tallinn, Estonia
[c] Department of Materials Science and Solar Energy Research Center (MIB-SOLAR), University of Milano-Bicocca, Via Cozzi 55, I-20125 Milano, Italy

ARTICLE INFO

Keywords:
Cu_2ZnSnS_4
Photoluminescence
Donor-acceptor pairs
Defects
Kesterites

ABSTRACT

We present photoluminescence (PL) studies of high quality Cu_2ZnSnS_4 single crystals and thin films. At T = 10 K two PL bands (D_1 and D_2) were detected in both samples at about 1.35 eV and 1.27 eV. The temperature and laser power dependencies indicate that the properties of PL bands can be explained by deep donor-deep acceptor pair model, where the D_1 and D_2 bands result from a recombination between pairs of the closest neighbors, and between pairs of the next-closest neighbors, respectively. The donor defect in these pairs is suggested to be an interstitial Zn atom and located in either of the two possible interstitial positions. The most probable deep acceptor defect in this pair is Cu_{Zn}.

1. Introduction

The kesterites Cu_2ZnSnS_4 (CZTS) and $Cu_2ZnSnSe_4$ (CZTSe) are attracting extensive interest as cheaper absorber materials for solar cells because first principles calculations predict that their electronic properties must be similar to more expensive chalcopyrite $Cu(In,Ga)Se_2$ (CIGSe) compounds, which already have shown quite high solar cell efficiency exceeding 22% [1]. However, the highest solar cell efficiency published for kesterites is only 12.6% [2]. To further improve the conversion efficiency of indium free kesterite solar cells, it is important to get more detailed information about different defects in CZTS-based materials. Photoluminescence (PL) spectroscopy is a powerful optical method for the characterization of defects in many semiconductor materials. Unfortunately, even the low temperature ($T \sim 10$ K) PL emission in CZTS usually shows a wide and single asymmetrical PL band at around 1.3 eV often affected by conduction and valence band tails [3–8]. These tails are created due to high concentration of different charged defects and the main recombination path often goes through these tails giving very little information about particular defects. At the same time, the PL band at 1.3 eV has shown somewhat different properties in different CZTS samples. In Ref [4], for example, it was found that the PL emission at 1.3 eV in slightly Cu-rich CZTS polycrystals consists of two PL bands at 1.27 eV and 1.35 eV that both result from band-to-deep acceptor (E_a = 280 meV) recombination in disordered and ordered CZTS, respectively. On the other hand, for the same PL band in CZTS, very different thermal quenching activation energies 48 meV [9], 39 meV and 59 meV [10], 29–40 meV [11] and 140 meV [12] have been also reported. Rather low activation energies and rather deep PL band ($E_g \sim 1.64$ eV at T = 10 K [13]) suggest that in many cases defect complexes are involved in the recombination process. Theoretical calculations have also shown that the formation of various defect complexes is highly probable in CZTS [14–18]. In our previous study [6], we showed that the recombination between electrons and holes in a quantum well, caused by the defect clusters that induce a significant local band gap decrease of 0.35 eV in CZTS, is characterized by a relatively low ($E_a < 100$ meV) thermal quenching activation energy. Also the quasi donor-acceptor pair (QDAP) model is often proposed to support the 1.3 eV PL band in CZTS [19–21]. Moreover, the peak position of this PL band depends on fraction of disordered kesterite phase in CZTS [5]. Usually in disordered structure the PL peak is red-shifted about 100 meV due to smaller band gap energy [4,22]. Therefore the presence of partial disordering can cause also spatial band gap energy fluctuations. So the varying behavior of the 1.3 eV PL band can be explained by different recombination mechanisms in samples with different chemical and structural composition although the PL emission falls into the same spectral region. One reason for this diversity is the variable quality of studied thin films or crystals. Almost all experimental studies on CZTS have shown that this absorber material has a very high concentration of charged point defects and these defects are responsible for the spatial electrostatic potential fluctuations. Relatively deep potential fluctuations and possible band gap energy fluctuations determine also the width (and shape) of PL bands and even at very low temperatures it is difficult to resolve all possible recombinations. The average depth of potential fluctuations γ (determined from the low-energy side of the PL band) in CZTS is about 50 meV [3,23,24], but γ values as low as 11 meV [4] and 22 meV [5]

* Corresponding author at: Department of Materials and Environmental Technology, Tallinn University of Technology, Ehitajate Tee 5, 19086 Tallinn, Estonia.
E-mail address: Juri.Krustok@ttu.ee (J. Krustok).

https://doi.org/10.1016/j.mssp.2018.02.025
Received 20 November 2017; Received in revised form 5 February 2018; Accepted 17 February 2018

were also reported. Therefore, it is obvious that for better understanding of PL processes samples with $\gamma < 25$ meV must be used.

In this report we present PL studies of high quality CZTS single crystal (SC) grown by iodine transport and CZTS thin film (TF) prepared by using sol-gel technology and show, that the PL emission at 1.3 eV in both samples involves two bands related to deep donor- deep acceptor pairs with different distance between donor and acceptor defects.

2. Experimental

The Cu_2ZnSnS_4 single crystals were grown via chemical vapor transport using iodine as a transport agent. Previously synthesized $Cu_{1.82}Zn_{1.12}SnS_{3.97}$ powder (3 N purity) was mixed together with 4 N purity CuI (5 mg of iodine per cm^3) and sealed in evacuated quartz ampoule. The sealed ampoule was placed in a two-zone horizontal furnace. Both temperature zones were heated up to 600 °C with the heating rate 2 °C/min and maintained at this temperature for 24 h. After that the temperatures at source and growth zones were raised up to 750 and 650 °C with the heating rate 2 °C/min, respectively. Crystal growth process took place at these temperature regimes for 2 weeks. After this, both zones were cooled down to room temperature (RT) with the cooling rate 3 °C/min. The chemical formula of single crystals calculated from EDX analysis data was $Cu_{1.87}Zn_{1.02}SnS_{3.87}$.

The sol-gel for CZTS thin films was prepared in a reaction flask by dissolving copper (II)-acetate monohydrate (2 N purity, 0.25 M), tin(II)-chloride dihydrate (2 N purity, 0.125 M), zinc(II)-acetate dihydrate (4 N purity, 0.125 M) and thiourea (2 N purity, 2.5 M) into dimethyl sulfoxide (3 N purity) by magnetic stirring for overnight at RT. Then the cap was removed and the solution left to rest until full gel formation. The resulting white and opaque gel was deposited onto a fluorine-doped tin oxide coated glass via doctor blade coating, using a Kapton tape mask; the resulting film was first annealed at 200 °C onto a hot-plate for 30 min (heating rate 3 °C/min) under nitrogen flow, subsequently the tape was removed and the layer sintered in oven under argon flow at 550 °C for 30 min (heating rate 2 °C/min). The sample was slowly cooled down in the furnace and stream of argon was turned off at 280 °C. The chemical formula of CZTS thin film calculated from EDX analysis data was $Cu_{2.02}Zn_{1.07}SnS_{4.02}$.

Raman spectra were recorded by using a Horiba's LabRam HR800 spectrometer and 532 nm laser line that was focused on the sample with spot size of about 5 μm. A 0.64 m focal length single grating (600 mm^{-1}) monochromator and the 442 nm line of a He-Cd laser with different power were used for the photoluminescence measurements. A closed-cycle helium cryostat was employed to measure temperature dependencies of the PL spectra at temperatures from 10 K to 300 K. The PL signal was detected by an InGaAs detector.

3. Results and discussion

Fig. 1(a) presents room temperature Raman spectra of both CZTS samples. Raman peak parameters were determined by fitting spectra with Lorentzian curves. The main A_1 peak of TF sample at 339 cm^{-1} has a halfwidth of $W = 2.7$ cm^{-1} and this quite small value verifies a good quality of CZTS. The halfwidth of the same peak in SC sample was slightly higher: $W = 3.8$ cm^{-1}. The presence of a small additional Raman peak at 335 cm^{-1} giving a shoulder to the CZTS A_1 peak at 339 cm^{-1} is observed in both samples and this peak is believed to be related to disordered kesterite phase in CZTS [4,25]. Again, the relative intensity of the 335 cm^{-1} peak was higher in SC sample. This small difference between TF and SC samples is probably related to a slightly different cooling rate after high temperature treatment of both samples. Although the slow cooling rate after the growth must result in an ordered phase [5], we are still able to detect a small fraction of disordered CZTS. The disordered kesterite phase typically involves a high concentration of antisite defects like Cu_{Zn} or Zn_{Cu} [26,27]. No other phases were detected by Raman measurements.

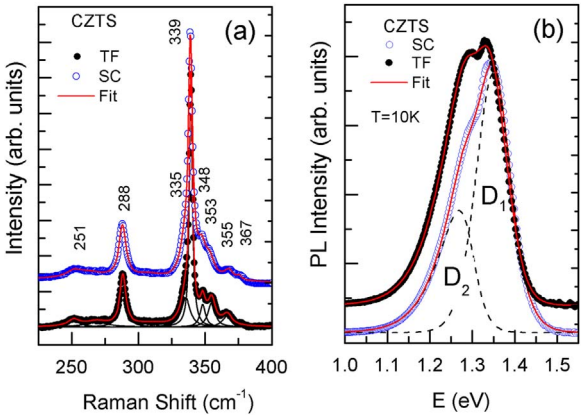

Fig. 1. (a) Room temperature Raman spectra and (b) low temperature PL spectra of CZTS single crystal (SC) and thin film (TF) samples together with fitting results (red lines). Spectra are vertically shifted for clarity.

Fig. 1(b) shows typical PL spectra of SC and TF CZTS at $T = 10$ K. Two asymmetric PL bands D_1 and D_2 are clearly visible at about 1.35 eV and 1.27 eV, respectively. All PL spectra were fitted using asymmetric double sigmoidal function [28] and the fitting result for SC sample is also shown in Fig. 1(b). The average depth of the potential fluctuations γ was determined from the exponential slope of the low-energy side of PL bands and was found to be around 25 meV for both samples. The separation between D_1 and D_2 PL bands was about 80 meV. The high-energy band (D_1) in both samples shows more rapid quenching with temperature, see Fig. 2(a). Arrhenius plots of the resulting integral intensities for both bands of SC sample are shown in Fig. 2(b). The best fits have been achieved for a single recombination channel and assuming a temperature dependence of the hole capture cross section proposed in [29]: $I(T) = I/[1 + A_1T^{3/2} + A_2T^{3/2} exp(-E_a/kT)]$, where I is the integral intensity of the PL band, A_1 and A_2 are process rate parameters and E_a is the activation energy. Obtained activation energies for D_1 and D_2 bands in SC sample were $E_a = 105$ meV and $E_a = 125$ meV, respectively. Thin film sample showed quite similar behavior with temperature. Although the double peak structure of the PL emission seems to be very similar to the structure reported in [4], the temperature dependence of this PL emission is different. Both PL bands in Ref. 4 showed very high temperature quenching activation energy $E_a \sim 280$ meV and the laser power dependence of the low-temperature PL spectrum revealed a strong blue shift of 15 meV per decade of both bands. In the present case such a strong blue shift was not observed, see Fig. 3(a). On the contrary, we observe very small red shift (≤ 2 meV per decade) for both bands and therefore it is obvious that D_1 and D_2 PL bands in our samples have different origin. Very similar D_1 and D_2

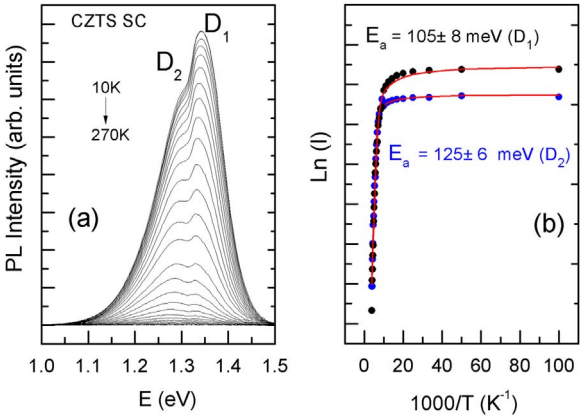

Fig. 2. (a) Temperature dependence of PL bands; (b) Arrhenius plots of integral intensity for D_1 and D_2 PL bands with fitting results of CZTS SC sample.

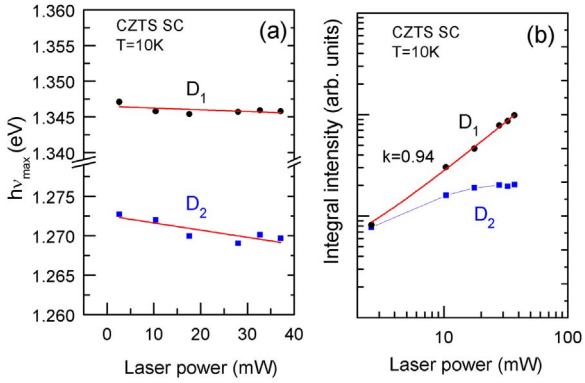

Fig. 3. Laser power dependencies of PL bands peak positions (a) and integral intensity (b) of CZTS SC sample.

peaks were recently observed also in ordered Cu_2CdSnS_4 samples, where the thermal activation energies of D_1 and D_2 PL bands were 60 meV and 110 meV, respectively and the separation between D_1 and D_2 PL bands in Cu_2CdSnS_4 was also 80 meV [30].

The double peak structure and properties of both bands suggest that these bands could be related to deep donor-deep acceptor (DD-DA) complex defect. The DD-DA pairs model was proposed to explain deep PL bands in CdTe [31] and in various chalcopyrites [32–34]. A detailed discussion about the DD-DA model is already published in [32,33]. Here we present only a short overview. According to this model double deep PL bands arise from a donor-acceptor recombination between pairs of the nearest neighbors (D_1-band), and between pairs of the next-nearest neighbors (D_2-band), respectively. It is known that the emission energy from a donor-acceptor (DA) pair with single charged components separated by a distance r is obtained from [35]:

$$E(r) = E_g - (E_A^0 + E_D^0) + \frac{e^2}{\varepsilon r} - \Gamma(r) \quad (1)$$

Here E_g is the band gap energy, $E_A{}^0$ and $E_D{}^0$ the acceptor and donor ionization energies, ε is the dielectric constant and $\Gamma(r)$ is an additional term including van der Waals and polarization interactions relevant at very short distances only. It is known, that the magnitude of $\Gamma(r)$ may exceed 25 meV or even more in case of very short donor-acceptor distances [35]. The correct value for the dielectric constant ε in case of very close pairs is quite difficult to calculate, but it is obvious, that in compound semiconductors ε must be a combination of both optical and static dielectric constants. Therefore Eq. (1) must be considered as a very rough method to calculate the transition energy of close DA pairs. However, for very close pairs, where $\Gamma(r_1) \approx \Gamma(r_2)$, the energy separation ΔE between the DA pairs of the nearest or the next-nearest neighbors can be calculated as follows:

$$\Delta E = \frac{e^2}{\varepsilon}\left(\frac{1}{r_1} - \frac{1}{r_2}\right) \quad (2)$$

In Eq. (2) r_1 is the shortest donor-acceptor distance and r_2 the next shortest one. It is important, that ΔE is not affected by spatial potential or/and band gap energy fluctuations, which determine mainly the width of PL bands.

It is also known that the electron (hole) wave function in the deep donor (acceptor) level must be highly localized. Therefore, for more distant pairs, there is practically no overlap of carriers wave functions and, consequently, no observable recombination emission. However, in some chalcopyrites PL bands (D_3-D_6) corresponding to larger distances between donor and acceptor defects were revealed [34]. In crystals donor and acceptor defects can occupy only certain lattice or intersitial positions. Our calculations, based on Eq. (2), indicate that in order to satisfy experimentally observed $\Delta E \approx 80$ meV, one of the DA pair components must be at an interstitial position (i) and the other one is at a lattice site, next to it. We used the lattice parameters $a = 0.5434$ nm, $c = 1.0838$ [36] for CZTS. Value $\varepsilon = 10.1$ was chosen in calculations in order to match experimentally determined energy separation between D_1 and D_2 bands and it stands between reported values $\varepsilon_0 = 11.6$ and $\varepsilon_\infty = 8$ for CZTS [37]. Calculated shortest DD-DA pair distances and PL bands peak positions are given in Table 1.

Table 1
Calculated shortest DD-DA pair distances and PL bands peak positions.

PL band	Cu-i distance	Interstitial position	$r_{D\text{-}A}$ (nm)	$\frac{e^2}{\varepsilon r}$ (eV)	Theoretical peak position (eV)
D_1	$(a^2/8 + c^2/64)^{1/2}$	T	0.2351	0.6064	1.350
D_2	c/4	O	0.2710	0.5262	1.270
	a/2	O	0.2717	0.5247	1.268

Due to tetragonal distortion ($c < 2a$) of a kesterite lattice, the D_2 peak is actually split, but the splitting is only 2 meV and it is impossible to detect this experimentally. The kesterite lattice has two types of interstitial positions with octahedral (O) and tetrahedral (T) symmetry. The first one (O) is surrounded by six cation (Cu, Zn and Sn) sites and the second one (T) by four cation sites, respectively. According to calculated defect formation energies in CZTS [14–18], the formation probability of interstitial donor defects Cu_i, Zn_i and Sn_i is quite small. However, the formation energy of different complex defects including interstitial defects is significantly lower and therefore the concentration of these complexes could be quite high. The Cu_i donor is considered as relatively shallow defect [14] and does not fit into our model. Single Sn_i donor has extremely high formation energy [13] and even when paired with some acceptor defect the formation of these defect complexes is very unlikely. Thus, the most probable isolated interstitial donor is Zn_i having quite deep energy level E_D^0 at about 400 meV below the conduction band edge in CZTS [15]. The corresponding acceptor defect must have a binding energy slightly higher than the thermal activation energy of D_2 band, i.e. $E_A^0 \geq 125$ meV. The most probable acceptor defect having the binding energy near this value is Cu_{Zn} [14,15]. Formation of Cu_{Zn}-Zn_i pairs, where the donor defect is deeper than the acceptor defect results to a more pronounced shift of donor level with decreasing distance between donor and acceptor defects [35]. This is why the separation between D_1 and D_2 PL bands is bigger than the difference between thermal activation energies for same bands.

It is a well-established fact that, as a rule, the recombination rate of DA pairs exponentially increases with decreasing the separation between donors and acceptors. This fact usually leads to the well-known j-shift of the DA PL bands, when the PL band maximum shifts towards higher energy with increasing laser power because more distant pairs saturate more easily. At the same time the peak positions of D_1 and D_2 PL bands do not show notable blue shift with increasing laser power. However, in case of very close DA pairs, when we are able to measure PL bands with discrete separation between donor and acceptor defects, different recombination rates of these close DA pairs result in different behavior of PL bands intensity on laser power. Therefore, the relative intensity of the closer-pair PL band D_1, situated at higher energy, should increase with laser power, while the intensity of D_2 band with a smaller recombination rate must start to saturate at higher laser power. Indeed, this can be seen in Fig. 3(b), where the intensity of D_1 band shows nearly linear increase with laser power ($k = 0.94$) and the D_2 band saturates at higher laser power. Only very small red shift of both PL bands with laser power can be seen in Fig. 3(a). This red shift could be related to slightly increased sample surface temperature at higher laser powers leading to a decrease of band gap energy E_g and/or could be also a result of imprecise spectral fitting due to relatively low intensity of D_2 PL band.

A final DD-DA recombination model for CZTS is given in Fig. 4. The observed double peak structure of the 1.3 eV PL band in CZTS is a clear indication that, in certain conditions, it is possible to reduce

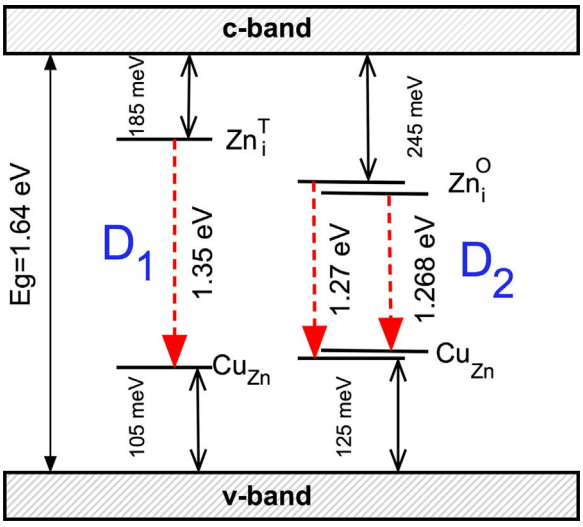

Fig. 4. DD-DA pairs model for CZTS at T = 10 K.

inhomogeneous broadening in kesterites and get valuable information about different defects using PL. While the antisite Cu_{Zn} acceptor defect is quite common in kesterites, the presence of interstitial donor defect Zn_i and DD-DA pairs Cu_{Zn} - Zn_i is not previously widely discussed. Further studies are needed in order to find methods to reduce a concentration of these harmful neutral complexes in kesterites.

4. Conclusions

A systematic study of the deep PL bands in CZTS single crystal and thin film samples was carried out. In both of these samples we found a very similar double deep emission bands D_1 and D_2. It was found that the experimental results for D_1 and D_2 PL emissions could be consistently explained by a DD-DA model. In this model the D_1 and D_2 bands are formed as a recombination between pairs of the closest neighbors, and between pairs of the next-closest neighbors, respectively. It is further concluded that the donor defect in these pairs is probably an interstitial Zn atom, and located in either of the two possible interstitial positions. The deep acceptor defect in this DD-DA pair is Cu_{Zn}.

Acknowledgements

This work was supported by institutional research funding (IUT19-28) of the Estonian Ministry of Education and Research, by the European Union through the European Regional Development Fund, Project TK141, by FP7 Project CHEETAH Grant Agreement No. 609788, and by University of Milano- Bicocca with the grant “Fondo di ateneo quota competitiva” project No. 2016-ATESP-0582.

References

[1] Zentrum für Sonnenenergie- und Wasserstoff-Forschung Baden- Württemberg (ZSW), ZSW Sets New World Record for Thin-film Solar Cells (Press Release09/2016).
[2] W. Wang, M.T. Winkler, O. Gunawan, T. Gokmen, T.K. Todorov, Y. Zhu, D.B. Mitzi, Device characteristics of CZTSSe thin-film solar cells with 12.6% efficiency, Adv. Energy Mater. 4 (2014) 1301465.
[3] M. Grossberg, J. Krustok, J. Raudoja, K. Timmo, M. Altosaar, T. Raadik, Photoluminescence and Raman study of Cu2ZnSn(SexS1-x)4 monograins for photovoltaic applications, Thin Solid Films 519 (2011) 7403–7406.
[4] M. Grossberg, J. Krustok, J. Raudoja, T. Raadik, The role of structural properties on deep defect states in Cu2ZnSnS4 studied by photoluminescence spectroscopy, Appl. Phys. Lett. 101 (2012) 102102.
[5] M. Grossberg, J. Krustok, T. Raadik, M. Kauk-Kuusik, J. Raudoja, Photoluminescence study of disordering in the cation sublattice of Cu2ZnSnS4, Curr. Appl. Phys. 14 (2014) 1424–1427.
[6] M. Grossberg, T. Raadik, J. Raudoja, J. Krustok, Photoluminescence study of defect clusters in Cu2ZnSnS4 polycrystals, Curr. Appl. Phys. 14 (2014) 447–450.
[7] X. Li, H. Cao, Y. Dong, F. Yue, Y. Chen, P. Xiang, L. Sun, P. Yang, J. Chu, Investigation of Cu2ZnSnS4 thin films with controllable Cu composition and its influence on photovoltaic properties for solar cells, J. Alloy. Compd. 694 (2017) 833–840.
[8] K. Tanaka, T. Shinji, H. Uchiki, Photoluminescence from Cu2ZnSnS4 thin films with different compositions fabricated by a sputtering-sulfurization method, Sol. Energy Mater. Sol. Cells 126 (2014) 143–148.
[9] K. Tanaka, Y. Miyamoto, H. Uchiki, K. Nakazawa, H. Araki, Donor-acceptor pair recombination luminescence from Cu 2ZnSnS4 bulk single crystals, Phys. Status Solidi (a) 203 (2006) 2891–2896.
[10] Y. Miyamoto, K. Tanaka, M. Oonuki, N. Moritake, H. Uchiki, Optical properties of Cu2ZnSnS4 thin films prepared by sol-gel and sulfurization method, Jpn. J. Appl. Phys. 47 (2008) 596–597.
[11] J.P. Leitão, N.M. Santos, P.A. Fernandes, P.M.P. Salomé, A.F. Da Cunha, J.C. González, G.M. Ribeiro, F.M. Matinaga, Photoluminescence and electrical study of fluctuating potentials in Cu2ZnSnS4-based thin films, Phys. Rev. B 84 (2011) 024120.
[12] S. Levcenko, V.E. Tezlevan, E. Arushanov, S. Schorr, T. Unold, Free-to-bound recombination in near stoichiometric Cu2ZnSnS4 single crystals, Phys. Rev. B 86 (2012) 45206.
[13] P.K. Sarswat, M.L. Free, A study of energy band gap versus temperature for Cu2ZnSnS4 thin films, Physica B 407 (2012) 108–111.
[14] S. Chen, J.H. Yang, X.G. Gong, A. Walsh, S.H. Wei, Intrinsic point defects and complexes in the quaternary kesterite semiconductor Cu2ZnSnS4, Phys. Rev. B 81 (2010) 35–37.
[15] S. Chen, A. Walsh, X.G. Gong, S.H. Wei, Classification of lattice defects in the kesterite Cu2ZnSnS4 and Cu2ZnSnSe4 earth-abundant solar cell absorbers, Adv. Mater. 25 (2013) 1522–1539.
[16] S. Chen, L.W. Wang, A. Walsh, X.G. Gong, S.H. Wei, Abundance of CuZn + SnZn and 2CuZn + SnZn defect clusters in kesterite solar cells, Appl. Phys. Lett. 101 (2012) 223901.
[17] D. Mutter, S.T. Dunham, Calculation of defect concentrations and phase stability in Cu2ZnSnS4 and Cu2ZnSnSe4 from stoichiometry, IEEE J. Photovolt. 5 (2015) 1188–1196.
[18] D. Huang, C. Persson, Band gap change induced by defect complexes in Cu2ZnSnS4, Thin Solid Films 535 (2013) 265–269.
[19] T. Gershon, B. Shin, N. Bojarczuk, T. Gokmen, S. Lu, S. Guha, Photoluminescence characterization of a high-efficiency Cu2ZnSnS4 device, J. Appl. Phys. 114 (2013) 2011–2016.
[20] X. Lin, A. Ennaoui, S. Levcenko, T. Dittrich, J. Kavalakkatt, S. Kretzschmar, T. Unold, M.C. Lux-Steiner, Defect study of Cu2ZnSn(SxSe1-x)4 thin film absorbers using photoluminescence and modulated surface photovoltage spectroscopy, Appl. Phys. Lett. 106 (2015) 013903.
[21] S. Levcenko, J. Just, A. Redinger, G. Larramona, S. Bourdais, G. Dennler, A. Jacob, T. Unold, Deep defects in Cu2ZnSn(*S*,Se)4 solar cells with varying Se content, Phys. Rev. Appl. 5 (2016) 024004.
[22] M. Valentini, C. Malerba, F. Menchini, D. Tedeschi, A. Polimeni, M. Capizzi, A. Mittiga, Effect of the order-disorder transition on the optical properties of Cu2ZnSnS4, Appl. Phys. Lett. 108 (2016) 211909.
[23] L. Yin, G. Cheng, Y. Feng, Z. Li, C. Yang, X. Xiao, Limitation factors for the performance of kesterite Cu_2ZnSnS_4 thin film solar cells studied by defect characterization, RSC Adv. 5 (2015) 40369–40374.
[24] L.Q. Phuong, M. Okano, G. Yamashita, M. Nagai, M. Ashida, A. Nagaoka, K. Yoshino, Y. Kanemitsu, Free-carrier dynamics and band tails in Cu2ZnSn(SxSe1-x)4: evaluation of factors determining solar cell efficiency, Phys. Rev. B 92 (2015) 115204.
[25] M.Y. Valakh, V.M. Dzhagan, I.S. Babichuk, X. Fontane, A. Perez-Rodriquez, S. Schorr, Optically induced structural transformation in disordered kesterite Cu2ZnSnS4, JETP Lett. 98 (2013) 255–258.
[26] J.J.S. Scragg, L. Choubrac, A. Lafond, T. Ericson, C. Platzer-Björkman, A low-temperature order-disorder transition in Cu2ZnSnS4 thin films, Appl. Phys. Lett. 104 (2014) 041911.
[27] S. Schorr, The crystal structure of kesterite type compounds: a neutron and X-ray diffraction study, Sol. Energy Mater. Sol. Cells 95 (2011) 1482–1488.
[28] J. Krustok, H. Collan, M. Yakushev, K. Hjelt, The role of spatial potential fluctuations in the shape of the PL bands of multinary semiconductor compounds, Phys. Scr. T79 (1999) 179–182.
[29] J. Krustok, H. Collan, K. Hjelt, Does the low-temperature Arrhenius plot of the photoluminescence intensity in CdTe point towards an erroneous activation energy? J. Appl. Phys. 81 (1997) 1442–1445.
[30] M. Pilvet, M. Kauk-Kuusik, M. Grossberg, T. Raadik, V. Mikli, R. Traksmaa, J. Raudoja, K. Timmo, J. Krustok, Modification of the optoelectronic properties of Cu2CdSnS4 through low-temperature annealing, J. Alloy. Compd. 723 (2017) 820–825.
[31] J. Krustok, H. Collan, K. Hjelt, J. Mädasson, V. Valdna, Photoluminescence from deep acceptor-deep donor complexes in CdTe, J. Lumin. 72–74 (1997) 103–105.
[32] J. Krustok, J.H. Schön, H. Collan, M. Yakushev, J. Mädasson, E. Bucher, Origin of the deep center photoluminescence in CuGaSe2 and CuInS2 crystals, J. Appl. Phys. 86 (1999) 364–369.
[33] J. Krustok, J. Raudoja, M. Krunks, H. Mändar, H. Collan, Nature of the native deep localized defect recombination centers in the chalcopyrite and orthorhombic AgInS2, J. Appl. Phys. 88 (2000) 205–209.
[34] J. Krustok, J. Raudoja, J.H. Schön, M. Yakushev, H. Collan, Role of deep donor-deep acceptor complexes in CIS-related compounds, Thin Solid Films 361–362 (2000) 406–410.
[35] F. Williams, Donor—acceptor pairs in semiconductors, Phys. Status Solidi 25 (1968) 493–512.
[36] L. Choubrac, A. Lafond, C. Guillot-Deudon, Y. Moelo, S. Jobic, Structure flexibility of the Cu2ZnSnS4 absorber in low-cost photovoltaic cells: from the stoichiometric to the copper-poor compounds, Inorg. Chem. 51 (2012) 3346–3348.
[37] C. Persson, R. Chen, H. Zhao, M. Kumar, D. Huang, Electronic structure and optical properties from first-principles modeling, Copper Zinc Tin Sulfide-Based Thin-Film Solar Cells, John Wiley & Sons Ltd, Chichester, UK, 2015, pp. 75–105.